THE JOURNAL OF BIOLOGICAL CHEMISTRY
Vol. 276, No. 52, Issue of December 28, pp. 49267–49274, 2001
Printed in U.S.A.

Gβ Association and Effector Interaction Selectivities of the Divergent Gγ Subunit $G\gamma_{13}$*

Received for publication, July 12, 2001, and in revised form, October 19, 2001
Published, JBC Papers in Press, October 23, 2001, DOI 10.1074/jbc.M106565200

Bonita L. Blake‡, Michele R. Wing, Janice Y. Zhou§, Qiubo Lei¶, Jennie R. Hillmann, Cynthia I. Behe, Rebecca A. Morris, T. Kendall Harden, Douglas A. Bayliss¶, Richard J. Miller§, and David P. Siderovski‖

From the Department of Pharmacology, University of North Carolina Neuroscience Center, and Lineberger Comprehensive Cancer Center, University of North Carolina, Chapel Hill, North Carolina 27599-7365, the §Department of Molecular Pharmacology and Biological Chemistry, Northwestern University, Chicago, Illinois 60611, and the ¶Department of Pharmacology, University of Virginia, Charlottesville, Virginia 22908-0735

$G\gamma_{13}$ is a divergent member of the Gγ subunit family considered to be a component of the gustducin G-protein heterotrimer involved in bitter and sweet taste reception in taste bud cells. $G\gamma_{13}$ contains a C-terminal asparagine-proline-tryptophan (NPW) tripeptide, a hallmark of RGS protein Gγ-like (GGL) domains which dimerize exclusively with $G\beta_5$ subunits. In this study, we investigated the functional range of $G\gamma_{13}$ assembly with Gβ subunits using multiple assays of Gβ association and Gβγ effector modulation. $G\gamma_{13}$ was observed to associate with all five Gβ subunits ($G\beta_{1-5}$) upon co-translation *in vitro*, as well as function with all five Gβ subunits in the modulation of Kir3.1/3.4 (GIRK1/4) potassium and N-type (α_{1B}) calcium channels. Multiple Gβ/$G\gamma_{13}$ pairings were also functional in cellular assays of phospholipase C (PLC) β2 activation and inhibition of $G\alpha_q$-stimulated PLCβ1 activity. However, upon cellular co-expression of $G\gamma_{13}$ with different Gβ subunits, only $G\beta_1/G\gamma_{13}$, $G\beta_3/G\gamma_{13}$, and $G\beta_4/G\gamma_{13}$ pairings were found to form stable dimers detectable by co-immunoprecipitation under high-detergent cell lysis conditions. Collectively, these data indicate that $G\gamma_{13}$ forms functional Gβγ dimers with a range of Gβ subunits. Coupled with our detection of $G\gamma_{13}$ mRNA in mouse and human brain and retina, these results imply that this divergent Gγ subunit can act in signal transduction pathways other than that dedicated to taste reception in sensory lingual tissue.

One major class of cellular signal transduction pathways is controlled by heterotrimeric guanine nucleotide-binding proteins ("G proteins"). The conventional model of heterotrimeric G-protein signaling involves serpentine cell-surface receptors (G protein-coupled receptors) coupled to a membrane-associated heterotrimer composed of a GTP-hydrolyzing Gα subunit and a Gβγ dimeric partner (1, 2). The WD-repeat β-propeller protein Gβ and the α-helical isoprenylated polypeptide Gγ form an obligate heterodimer that binds tightly to GDP-bound Gα, enhancing Gα coupling to receptor and inhibiting its release of GDP. Guanine nucleotide exchange activity of agonist-occupied G protein-coupled receptors facilitates dissociation of Gα·GTP and Gβγ subunits and allows both moieties to modulate a variety of downstream effectors; for the free Gβγ dimer, these effectors include the second messenger generators adenylyl cyclase and phospholipase C-β (PLCβ)[1] as well as ion channels such as G protein-coupled inward-rectifying potassium (GIRK) channels and N-type calcium channels (3, 4).

Considerable functional diversity is possible within the large combinatorial range of potential Gβγ dimers (5, 6), given the existence of at least six Gβ subunits ($G\beta_{1-4}$, the outlier $G\beta_5$, and its retinal-specific isoform $G\beta_{5L}$; Refs. 7 and 8) and 11 Gγ subunits (three farnesylated and eight geranylgeranylated species; Fig. 1). However, outside the unique nature of $G\gamma_1$ (the farnesylated Gγ of the retinal phototransduction cascade; Refs. 9–12), specific roles for particular Gγ subunits in the Gα- or effector-binding capacity of Gβγ remain elusive. The Gγ polypeptide is not thought to contribute to the interaction between Gβγ and Gα·GDP, based on analyses of atomic resolution structures of $G\alpha_t\beta_1\gamma_1$ and $G\alpha_{i1}\beta_1\gamma_2$ complexes (13–16). The particular isoprenyl lipid group attached to the Gγ C terminus, however, may modulate Gα-, receptor-, and/or effector-coupling efficiencies of Gβγ dimers (11, 12).

A divergent member of the Gγ subunit family, $G\gamma_{13}$, was recently cloned from mouse neuroepithelial taste receptor cells (17) and, independently, in a functional screen for mouse brain mRNAs that exert a growth inhibitory effect after expression in *Escherichia coli* (18). $G\gamma_{13}$ is unique in possessing an asparagine-proline-tryptophan (NPW) tripeptide prior to the C-terminal isoprenylation signal sequence; this conserved tripeptide ends in phenylalanine (*i.e.* NPF) in all other mammalian Gγ polypeptides. The NPW motif is also found within the Gγ-like (GGL) domains of the R7 subfamily of mammalian RGS proteins (RGS6, -7, -9, and -11; Fig. 1*B*). We and others recently have shown that GGL domains specify a uniquely selective association with $G\beta_5$ isoforms (reviewed in Ref. 19). Moreover, molecular modeling and mutagenesis of GGL domains and Gγ

* This work was supported in part by National Institutes of Health Grants GM62338 (to D. P. S.), NS33826 (to R. J. M.), NS39553 (to D. A. B.), and GM29536 (to T. K. H.). The costs of publication of this article were defrayed in part by the payment of page charges. This article must therefore be hereby marked "*advertisement*" in accordance with 18 U.S.C. Section 1734 solely to indicate this fact.

‡ Supported by a National Institute of Mental Health Career Development Award MH001896.

‖ Year 2000 Scholar of The EJLB Foundation and recipient of the Burroughs Wellcome Fund New Investigator Award in the Basic Pharmacological Sciences. To whom all correspondence should be addressed: Dept. of Pharmacology, CB#7365 UNC-Chapel Hill School of Medicine Mary Ellen Jones Building, Rm. 1106, Chapel Hill, NC 27599-7365. Tel.: 919-843-9363; Fax: 919-966-5640; E-mail: dsiderov@med.unc.edu.

[1] The abbreviations used are: PLC, phospholipase C; EST, expressed sequence tag; GFP, green fluorescent protein; GGL, Gγ-like domain; GIRK, G protein-coupled inwardly rectifying potassium; GTPase, guanosine triphosphatase; HA, hemagglutinin epitope tag; RGS, regulator of G-protein signaling; GAPDH, glyceraldehyde-3-phosphate dehydrogenase; RT, reverse transcriptase.

subunits (20, 21) led us to identify the NPW motif as a potentially critical component of the absolute selectivity of GGL/Gβ_5 interactions; we termed this the "Trp-274 hypothesis" (21). In this report, we describe the assembly of Gγ_{13} with Gβ isotypes and the functional range of these dimers in both Gα association and downstream effector activation. In particular, we address whether the Trp-274 hypothesis of exclusive Gβ_5 association holds true for this divergent Gγ subunit.

EXPERIMENTAL PROCEDURES

Expression Constructs—The entire open reading frame of mouse *Gγ$_{13}$* was amplified by PCR (sense primer 5′-GGGATCCGACGCCATGGAGGAGTGGGATG-3′, antisense primer 5′-GTCTAGAGTGTGGGTCAGGCTCATAGG-3′) from a Marathon™ mouse brain cDNA library (CLONTECH), digested with *Eco*RI and *Xba*I, and subcloned in-frame with an N-terminal tandem hemagglutinin (HA)-epitope tag into pcDNA3.1 (Invitrogen) as previously described (20). G protein β-subunit constructs with an N-terminal Myc-epitope tag, as well as wild-type and F61W mutant Gγ_2 expression constructs have previously been described (21, 22).

Reverse Transcription-Polymerase Chain Reaction (RT-PCR) and Northern Blot Analyses—Marathon™ cDNA pools from human heart, brain, spleen, retina, and lymph node poly(A)$^+$ mRNA (CLONTECH) were amplified by PCR using primer sets specific for human *Gγ$_{13}$* (sense primer 5′-TTGTCATTGTCCCTCCGCTGTCAC-3′, antisense primer 5′-GCTCACAGGATGGTGCATTTG-3′) and glyceraldehyde-3-phosphate dehydrogenase (*GAPDH;* sense primer 5′-GACCACAGTCCATGCCATCACT-3′, antisense primer 5′-TCCACCACCCTGTTGCTGTAG-3′) mRNAs. The 273-bp human brain *Gγ$_{13}$* PCR product, encoding the entire open reading frame, was cloned into the vector pCR2.1 using the TOPO-TA cloning kit (Invitrogen). An *Eco*RI fragment of this construct was labeled with [α-^{32}P]dATP (Amersham Bioscience Inc.) by random priming (StripEZ, Ambion), and hybridized under stringent conditions with a human brain multiple tissue Northern (MTN™) blot (CLONTECH) using the NorthernMax system (Ambion). A mouse tissue MTN™ blot was similarly hybridized with a ^{32}P-labeled 301-bp *Eco*RI/*Xba*I fragment of mouse *Gγ$_{13}$* cDNA. To control for RNA loading and quality, both MTN™ blots were also hybridized with a commercially available *GAPDH* cDNA probe (Ambion).

In Vitro Gβ/Gγ Co-translation and Immunoprecipitation—In vitro transcription and translation reactions were performed using the TNT™ reticulocyte lysate system (Promega). T7 promoter-based metabolic ^{35}S labeling of HA-tagged Gγ_{13} or Gγ_2(F61W) co-expressed with one of five Myc-tagged Gβ subunit expression vectors (Gβ_{1-5}) was performed as previously described (20, 21, 23). Briefly, Gγ proteins were immunoprecipitated (IP) using anti-HA monoclonal antibody 12CA5 (Roche Molecular Biochemicals) and protein A-Sepharose (Sigma) in Buffer D (50 mM NaCl, 10 mM $MgCl_2$, 50 mM Tris, pH 8.0, 1 mM EDTA, 10 mM β-mercaptoethanol, 20% glycerol, 0.05% $C_{12}E_{10}$). Immunoprecipitated complexes were washed three times with 0.4 ml of Buffer D. Co-precipitating [^{35}S]methionine-labeled Gβ and Gγ subunits were identified by SDS-PAGE on Novex 14% Tris-glycine gels (Invitrogen) followed by direct autoradiography.

Cellular Gβ/Gγ Co-immunoprecipitation—Detailed experimental procedures were provided previously (20, 21, 23) and only differences from published protocols are provided below. Transient co-transfections of HEK293T cell monolayers with Myc-tagged Gβ and HA-tagged Gγ expression constructs were performed using Effectene transfection reagent (Qiagen) according to the manufacturer's instructions. Transfected cells were harvested 48 h post-transfection by scraping into 1 ml of RIPA-150 buffer (150 mM NaCl, 50 mM Hepes, pH 7.5, 20 mM EDTA, 0.5% deoxycholate, 1% Nonidet P-40, 0.1% SDS, Complete™ Mini EDTA-free protease inhibitor mixture (Roche Molecular Biochemicals)). Lysates were prepared by passing cell suspension 10 times through a 23-gauge needle followed by centrifuging at 16,000 × *g* for 5 min at 4 °C to remove insoluble material. Supernatants were adjusted to 1 mg/ml total protein (concentrations measured using Bio-Rad D_C protein assay reagent) and precleared for 45 min with 20 μl of 50% (v/v) protein A/G-agarose beads (Santa Cruz). Following removal of beads by centrifugation at 10,000 × *g* for 1 min, the supernatants were transferred to fresh tubes containing anti-HA monoclonal antibody 12CA5 (Roche Molecular Biochemicals) and incubated with constant rotation for 1 h at 4 °C. The immune complexes were centrifuged, and the supernatants were transferred to fresh tubes containing 40 μl of 50% (v/v) protein A/G beads. The complexes were rotated at 4 °C for 1 h, and then centrifuged at 10,000 × *g* for 1 min to collect the beads. The protein A/G beads were washed twice in RIPA-500 buffer (21), followed by three washes in RIPA-150 buffer. Immunocomplexes were eluted from the beads by adding 50 μl of Laemmli sample buffer and boiling for 5 min. Proteins were separated on 12% SDS-PAGE gels and electroblotted onto polyvinylidene difluoride membranes (Millipore) for detection of Gβ subunits with anti-Myc mouse monoclonal antibody conjugated to horseradish peroxidase (9E10-HRP; Roche Molecular Biochemicals), followed by enhanced chemiluminescence (Amersham Bioscience, Inc.). Gγ subunits were detected using anti-HA rat monoclonal antibody 3F10-horseradish peroxidase (Roche Molecular Biochemicals).

GIRK Channel Electrophysiology—Transient transfection and electrophysiological recordings of the stable G1,4 cell line, a HEK293 derivative line expressing GIRK1 and GIRK4 potassium channel subunits, were performed as recently described (24). Briefly, Gβ and Gγ expression plasmids were co-transfected at a concentration of 6 μg each per 35-mm culture dish, along with 1 μg per dish pGreenLantern (Invitrogen), a plasmid encoding enhanced green fluorescent protein (GFP). Electrophysiological recordings were acquired and analyzed using an Axopatch 200A patch clamp amplifier and the pCLAMP program suite (Axon Instruments). Inwardly rectifying whole cell currents were evoked from cells held at −50 mV while applying a voltage ramp command at 0.1 Hz (Δ −90 mV; 0.1 V/s). Slope conductance was obtained from a linear fit to current voltage data over the range of −100 to −120 mV. Statistical analysis was performed using ANOVA, with *post-hoc* Bonferroni test. All GIRK channel data are presented as mean ± S.E., with $p < 0.05$ considered statistically significant.

N-type Ca^{2+} Channel Electrophysiology—Voltage-dependent inhibition of calcium channels by Gβγ subunit expression was studied in C2D7 cells, a HEK293-derivative line expressing human α_{1B} (N-type) Ca^{2+} channels (α_{1B}, $\alpha_2\delta$, and β_{1-3} subunits) (25). Cells were transiently transfected with 5 μg of Gβ and 5 μg of Gγ DNA, along with 1 μg of commercially available GFP vector (Invitrogen), as previously described (26). Cell culture, cell identification, and whole cell patch clamp of Ba^{2+} current ($n = 6\sim11$) were performed as previously described (26). Prepulse facilitation ratios, indicative of Gβγ-mediated, voltage-dependent inhibition, were calculated from these currents and analyzed as described by Simen and Miller (25). Multiple comparisons of calcium current results were performed using one-way ANOVA, followed by a nonparametric Kolmogorov-Smirnov test.

PLCβ2 Activation by Gβγ Subunits—COS-7 cells were maintained at 5% CO_2 in Dulbecco's modified Eagle's medium with high glucose and supplemented with 10% fetal calf serum and antibiotics. Approximately 24 h prior to transfection, cells were replated into 12-well plates at a density of 7.5×10^5 cells per well. Subconfluent cells were transfected using Fugene transfection reagent (Roche Molecular Biochemicals) with 300 ng of PLCβ2 vector, 200 ng each of appropriate Gβ and/or Gγ subunit expression vectors, and sufficient pcDNA3.1 vector to achieve 700 ng/well total DNA. After incubating 24 h with DNA and transfection reagent, the medium was removed and replaced with 400 μl of inositol-free and serum-free Dulbecco's modified Eagle's medium containing 1 μCi of *myo*-[^{3}H]inositol (American Radiolabeled Chemicals, Inc.). To initiate the accumulation of radiolabeled inositol phosphates, LiCl (10 mM final concentration) was added to the labeling medium and cells were incubated for 1 h at 37 °C. Medium was then aspirated and cells were lysed by adding ice-cold 50 mM formic acid and incubated on ice for 20 min. After neutralization with 250 μl of 150 mM NH_4OH, lysates were loaded onto Dowex ion exchange columns, and washed with 10 ml of water and 10 ml of 50 mM formic acid. Inositol phosphates were eluted with 5 ml of 1.2 M ammonium formate, 100 mM formic acid.

Gβγ Subunit Inhibition of $G\alpha_q$-stimulated PLCβ1 Activity—Gβγ subunit-mediated inhibition of Gαq-stimulated [^{3}H]inositol phosphate accumulation was measured as described above, except that COS-7 cells were transiently transfected with 20 ng of $G\alpha_q$ vector in addition to 300 ng of PLCβ1 vector, 200 ng each of the indicated Gβ and/or Gγ subunit expression vectors, and pcDNA3.1 vector DNA to a total of 720 ng/well.

RESULTS

In Silico Identification of Novel Gγ Sequences—In a continuing search for Gγ-like (GGL) polypeptide sequences (20), we employed the Simple Modular Architecture Research Tool (SMART; Ref. 27) to identify uncharacterized GGL sequences among anonymous open reading frames derived from eukaryotic genome sequencing projects. We recently reported the identification of two open reading frames from genes of the *Drosophila melanogaster* genome (CG15844 and CG18511) that possess GGL domains (19). The latter predicted polypep-

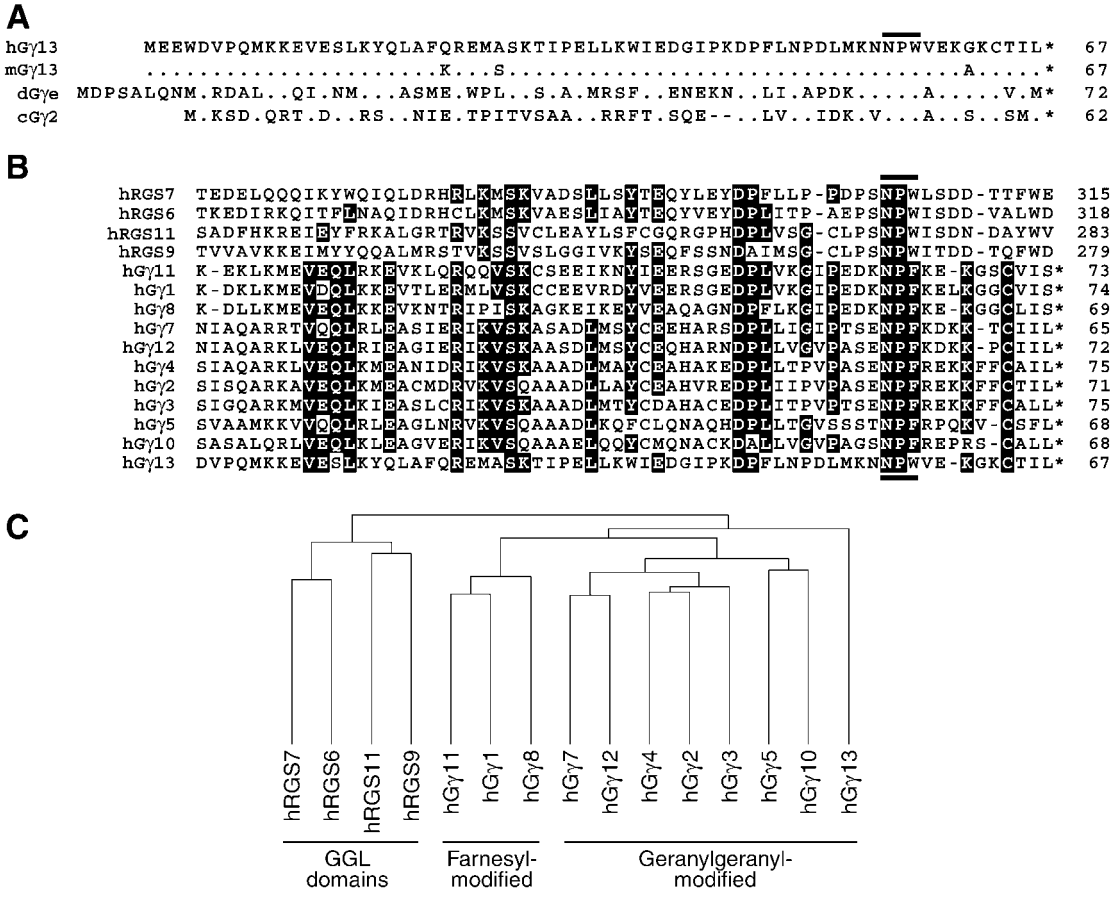

FIG. 1. **Sequence comparisons between $G\gamma_{13}$, other Gγ subunits, and GGL domains.** *A*, amino acid alignment of NPW-containing Gγ subunits from *Homo sapiens* (*h*), *Mus musculus* (*m*), *Drosophila melanogaster* (*d*), and *Caenorhabditis elegans* (*c*) (GenBank™ accession numbers 7706567, 11967949, 6782318, and 7498606, respectively). Identical amino acids are indicated by a *period* (.) and gaps with a *dash* (−). The end of the unprocessed polypeptide chain is denoted with an *asterisk* (*). NPW motif is *overlined*. *B*, multiple sequence alignment of human Gγ subunits and GGL domains of human RGS proteins. *Black boxes* depict identical amino acids shared by at least 60% of sequences within alignment; NPW motif shared between GGL domains and $G\gamma_{13}$ is *overlined* and *underlined*, respectively. *C*, pairwise sequence similarity relationships between human Gγ subunits and GGL domains as computed by the Wisconsin GCG Pileup program using default parameters. The $hG\gamma_{13}$ subunit is predicted to be geranylgeranylated based on the C-terminal leucine of the CAAX box sequence (45, 46). GenBank™ accession numbers for human sequences used: RGS7, 11140809; RGS6, 4972617; RGS11, 4506507; RGS9, 4506521; $G\gamma_{11}$, 4758448; $G\gamma_1$, 11386179; $G\gamma_8$, 3023844; $G\gamma_7$, 4826746; $G\gamma_{12}$, 10047118; $G\gamma_4$, 4758450; $G\gamma_2$, 11277005; $G\gamma_3$, 6912394; $G\gamma_5$, 4885287; $G\gamma_{10}$, 4758446; $G\gamma_{13}$, 7706567.

tide data base record (CG18511, also known in the Celera data base as CP42246; Ref. 28) is, in fact, an erroneous C-terminal sequence extension of a known Gγ subunit, the *Drosophila* visual Gγ subunit $G\gamma_e$ (29). More recently, we identified a GGL domain within a predicted 89-amino acid polypeptide computed from genomic DNA sequence of a 2-Mb span of human chromosome 16p13.3 (GenBank™ accession number AL031033; protein product C321D2.5); this predicted open reading frame data base record is also an erroneous sequence extension of a recently isolated human Gγ subunit, $G\gamma_{13}$ (17).

Alignment of the correct polypeptide sequences of human $G\gamma_{13}$ and *Drosophila* $G\gamma_e$, along with corresponding orthologs from mouse ($mG\gamma_{13}$; Ref. 18) and *C. elegans* ($cG\gamma_2$; Ref. 29), revealed 100% conservation of a unique asparagine-proline-tryptophan (NPW) tripeptide sequence at the C terminus prior to the CAA*X* box (Fig. 1*A*). While the presence of an NPW motif was found to be unique among conventional, isoprenylated Gγ subunits (*e.g.* comparing $hG\gamma_{13}$ to all other human Gγ subunits; Fig. 1*B*), this NPW motif is a hallmark of the internal GGL domains of R7 subfamily (or "C-subfamily") RGS proteins (20, 21). Pairwise comparisons of all human Gγ and GGL domain sequences (Fig. 1*C*) confirmed the divergent nature of the NPW motif-containing Gγ subunit.

Expression of $G\gamma_{13}$ in Neural Tissue—The human and mouse $G\gamma_{13}$ open reading frames were cloned using RT-PCR. cDNA pools from human and mouse whole brain and retinal tissues gave detectable RT-PCR products, whereas neither $G\gamma_{13}$ product was detected in lymph node, spleen, or heart cDNA samples (Fig. 2*A* and data not shown). The RT-PCR products from brain cDNA were cloned, sequence verified, and used as probes in Northern blot analyses of $G\gamma_{13}$ expression. Analysis of a mouse multiple tissue Northern blot revealed the expression of a ~0.5-kb murine $G\gamma_{13}$ transcript that was restricted to brain (Fig. 2*B*). The human $G\gamma_{13}$ mRNA was observed in whole brain as a single ~1.3-kb transcript (Fig. 2*C*) and, among several brain regions tested, was specifically expressed in the thalamus. These results are comparable to the brain-specific expression observed in complementary human multiple tissue and mouse brain subregion Northern blots by Huang and colleagues (17). In addition, serial analysis of gene expression maps and EST profiles of the human and mouse $G\gamma_{13}$ sequences (UniGene clusters Hs.247888 and Mm.45263; Ref. 30) also indicate a primarily brain-specific expression pattern. In total, these findings suggest that $G\gamma_{13}$ expression is limited primarily to sensory epithelia and neural tissues.

In Vitro and Cellular Assembly of Gβ/$G\gamma_{13}$ Dimers—We previously hypothesized that the NPW motif of GGL domains plays a critical role in the exclusive $G\beta_5$ association by R7 subfamily RGS proteins (21). We therefore tested the NPW motif-containing $G\gamma_{13}$ subunit for its Gβ association specificity.

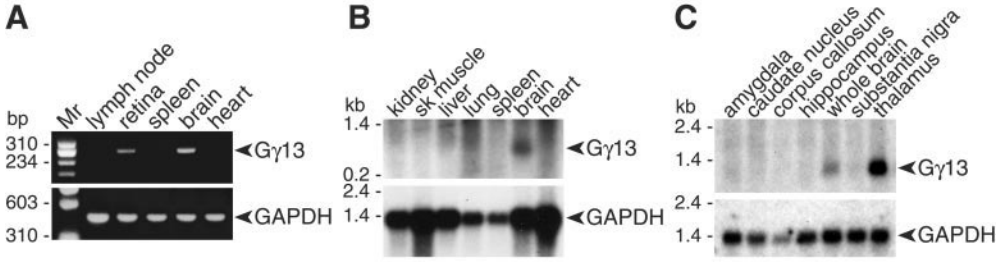

FIG. 2. **Expression profile of $G\gamma_{13}$ mRNA in human and mouse tissue samples.** *A*, cDNA pools from the indicated human poly(A)$^+$ RNA sources were PCR amplified using primer sets specific for human $G\gamma_{13}$ and GAPDH mRNAs. Predicted molecular weights of $G\gamma_{13}$ and GAPDH amplicons are 273 and 453 bp, respectively. "M_r" denotes DNA molecular weight standards. *B*, mouse multiple tissue Northern blot (2 μg of poly(A)$^+$ RNA per lane) was probed in sequential fashion with randomly primed ^{32}P-labeled mouse $G\gamma_{13}$ and GAPDH cDNA probes. "*Sk muscle*" denotes skeletal muscle mRNA lane. *C*, Northern blot of various human brain anatomical features (2 μg of poly(A)$^+$ RNA per lane) was probed in sequential fashion with randomly primed ^{32}P-labeled human $G\gamma_{13}$ and GAPDH cDNA probes.

T7 promoter-based expression vectors for HA epitope-tagged $G\gamma_{13}$ (or $G\gamma_2$(F61W) as a positive control; Ref. 21), along with one of five Myc-tagged Gβ subunit expression vectors ($G\beta_{1-5}$), were co-transcribed and translated in reticulocyte lysates as previously described (20, 21, 23). Gγ proteins were immunoprecipitated using anti-HA monoclonal antibody and the immunocomplexes were washed with low detergent conditions (0.05% $C_{12}E_{10}$) prior to detection of associated, [^{35}S]methionine-labeled Gβ subunits by SDS-PAGE and autoradiography. As previously reported (21), substituting tryptophan for phenylalanine in the NPF motif of $G\gamma_2$ (*i.e.* the "F61W" point mutation) facilitates $G\gamma_2$ dimerization with all five Gβ subunits (including $G\beta_5$) in low-detergent conditions (Fig. 3*A*, *left panel*). Similarly, co-translated $G\gamma_{13}$ bound to all five Gβ subunits in these low-detergent conditions (Fig. 3*A*, *right panel*).

To test $G\beta/G\gamma_{13}$ dimer assembly in a cellular context, expression vectors for HA-tagged $G\gamma_{13}$, $G\gamma_2$, or RGS11 proteins were transiently transfected into HEK293T cells, along with one of five Myc-tagged Gβ subunit expression vectors ($G\beta_{1-5}$). Lysates of transfected cells were immunoprecipitated with anti-HA antibody and immunoblotted with anti-Myc antibody to detect bound Gβ subunits. As shown in Fig. 3*B* (*right panel*), only $G\beta_1/G\gamma_{13}$, $G\beta_3/G\gamma_{13}$, and $G\beta_4/G\gamma_{13}$ dimers were detected in cellular lysates by co-immunoprecipitation. The apparent lack of detectable $G\gamma_{13}$ association with $G\beta_2$ and $G\beta_5$ in this experiment was not the result of deficient Gβ subunit expression levels (*i.e.* Fig. 3*B*, *Lysate Blot:anti-Myc*), nor the result of a functional deficiency in expressed $G\beta_2$ and $G\beta_5$ proteins, since the positive controls $G\gamma_2$ and RGS11 bound avidly to $G\beta_2$ and $G\beta_5$ subunits, respectively (Fig. 3*B*, *left panel*). These findings suggest that under the high-detergent conditions used for this cellular co-immunoprecipitation assay (*i.e.* RIPA buffer with 0.5% deoxycholate, 1% Nonidet P-40, and 0.1% SDS), $G\gamma_{13}$ remains stably associated with $G\beta_1$, $G\beta_3$, and $G\beta_4$, and is not, or is very weakly, associated with $G\beta_2$ and $G\beta_5$.

Modulation of K^+ Channels by $G\beta/G\gamma_{13}$ Pairs—The capacity of $G\gamma_{13}$, in combination with each of the Gβ subunits, to modulate GIRK currents was examined using whole cell patch clamp electrophysiology. G1,4 cells, stably expressing Kir3.1/3.4 (GIRK1/4) channels (24), were transiently transfected with GFP and empty vector (control) or GFP and Gβ/Gγ vector pairs. GIRK channel conductance in cells co-transfected with $G\gamma_{13}$ and one of the first four Gβ subunits ($G\beta_{1-4}$) was markedly enhanced (Fig. 4). The current activation elicited by Gβγ dimers consisting of $G\beta_{1-4}$ in combination with $G\gamma_{13}$ was not significantly different from that observed with cognate Gβγ dimers formed with $G\gamma_2$ (*e.g.* $\beta_1\gamma_{13}$ *versus* $\beta_1\gamma_2$; Fig. 4*A*). In contrast, G1,4 cells co-transfected with $G\gamma_{13}$ and $G\beta_5$ subunits displayed significantly diminished GIRK currents relative to vector-transfected cells (Fig. 4*B,* and *inset* of *C*); this observation is consistent with our previous report that $G\beta_5$ containing

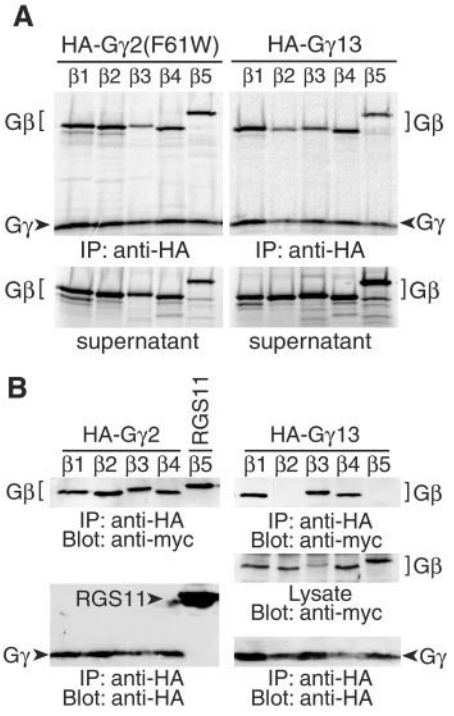

FIG. 3. **Gβ binding specificity of $G\gamma_{13}$ as measured by *in vitro* and cellular co-immunoprecipitations.** *A*, Gβ subunits were co-translated *in vitro* in reticulocyte lysates with HA-epitope tagged $G\gamma_2$(F61W) (*left panel*) or $G\gamma_{13}$ subunits (*right panel*). HA-tagged Gγ subunits were immunoprecipitated (*IP*) with anti-HA monoclonal antibody, washed under low detergent conditions (0.05% $C_{12}E_{10}$), and bound Gβ subunits were visualized by autoradiography after SDS-PAGE. Clarified supernatants were also visualized in the same manner to confirm uniform Gβ subunit expression. Results displayed are representative of three independent experiments. *B*, HEK293T cells were transiently co-transfected with expression vectors for HA-tagged $G\gamma_{13}$ (*right panel*), or $G\gamma_2$ or RGS11 as positive controls (*left panel*), along with one of five Myc-tagged Gβ subunit expression vectors (β_{1-5}). Cell lysates were immunoprecipitated (*IP*) with anti-HA mAb, and coimmunoprecipitating Gβ subunits were detected by immunoblotting (*Blot*) with anti-Myc monoclonal antibody. To discount lack of Gβ or Gγ expression as a trivial explanation for lack of observable $G\beta_2$ and $G\beta_5$ coimmunoprecipitation with $G\gamma_{13}$, cell lysates were directly immunoblotted for Gβ expression using anti-Myc monoclonal antibody (***"Lysate"***), and Gγ species were directly detected by anti-HA mAb immunoblotting (*lower panels*).

dimers $\beta_5\gamma_2$ and $\beta_5\gamma_{11}$ inhibit, rather than activate, GIRK1,4 and GIRK1,2 channels (24). Collectively, these findings suggest that $G\gamma_{13}$ associates nonselectively with *all* Gβ subunits to modulate GIRK channel currents.

Inhibition of N-type Calcium Channels by $G\beta/G\gamma_{13}$ Pairs—The HEK293-derived cell line C2D7 stably expresses human α_{1B} (N-type) Ca^{2+} channels and serves as a useful model for the

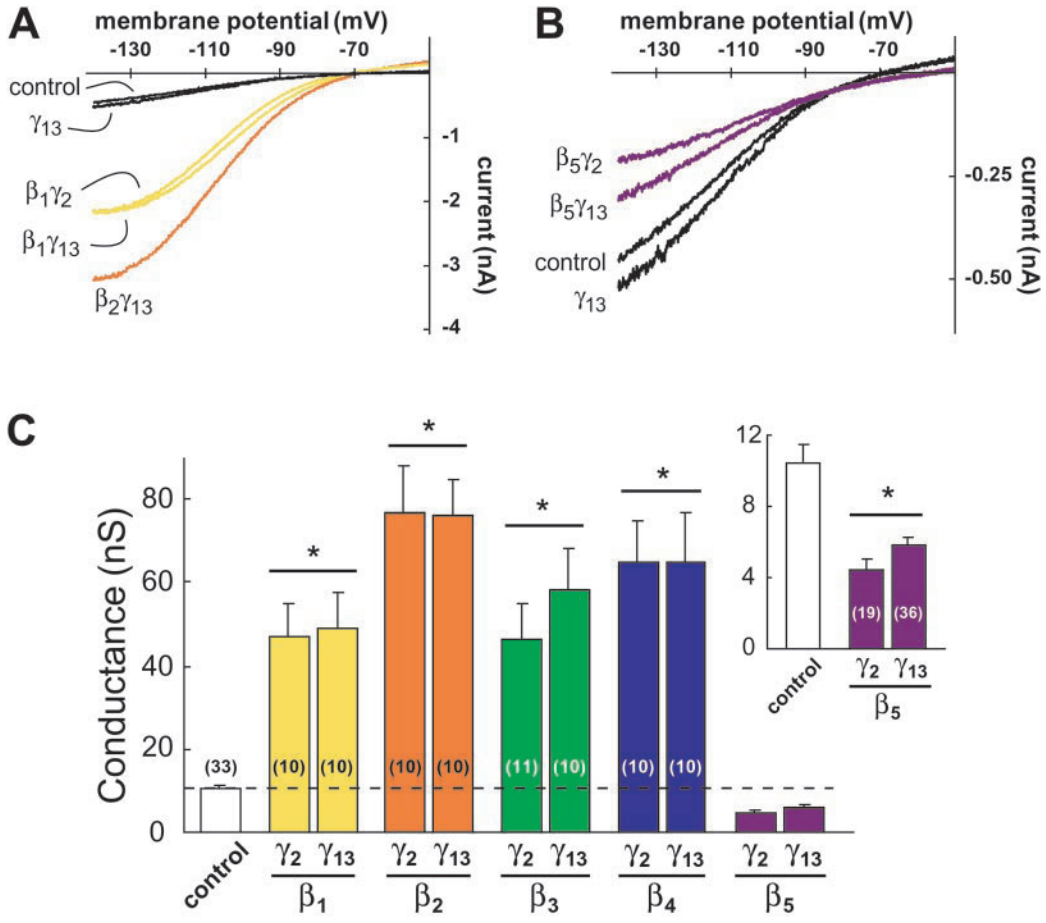

FIG. 4. **GIRK1/4 channel currents are modulated equivalently by Gβ/Gγ2 and Gβ/Gγ13 dimers.** *A* and *B* represent sample current traces from control cells (*i.e.* G1,4 cells transfected with GFP alone) and from G1,4 cells transiently transfected with the indicated Gβ and/or Gγ subunits. *C*, *bar graph* of averaged data (± S.E.) depicts the GIRK conductance in cells transfected with GFP and empty vector (*control*) or GFP and the indicated Gβγ pairs. As a measure of channel activity, peak whole cell conductance (nS) was determined by patch clamp recordings as the slope of a ramp I-V curve between −100 and −120 mV. *Numerals in parentheses* denote number of cells tested for each transfection paradigm. *Asterisks* denote statistically significant differences from control ($p < 0.05$ by ANOVA, with *post-hoc* Bonferroni test). As previously reported (Ref. 24), Gβ or Gγ subunits expressed alone have no significant effect on GIRK conductance: *e.g.* $G\beta_2$ alone = 10.5 ± 1.0 nS (14 cells), $G\gamma_2$ alone = 8.4 ± 1.0 nS (15 cells), and $G\gamma_{13}$ alone = 12.7 ± 2.0 nS (16 cells) *versus* empty vector = 9.9 ± 0.8 nS (33 cells). *Inset*, averaged data (± S.E.) from control and $G\beta_5$-expressing cells are shown on an expanded scale. As previously reported (24), $G\beta_5$-containing dimers *inhibit* Gβγ-stimulated GIRK channels.

study of G-protein subunit effects on Ca^{2+} channel activity (25, 26). To determine whether $G\gamma_{13}$ forms Gβγ dimers capable of modulating Ca^{2+} channel activity, C2D7 cells were transiently transfected with GFP and empty vector (control) or with GFP and combinations of individual Gβ subunits ($G\beta_{1-5}$) and HA-tagged $G\gamma_2$ or $G\gamma_{13}$. Total Ba^{2+} currents (I_{Ba}) were recorded from fluorescent cells in the whole cell configuration as previously described (26). As shown in Fig. 5 (*inset*), a test pulse to +10 mV (test pulse 1) elicited a biphasic I_{Ba} in vector-transfected control C2D7 cells consisting of a rapid activation phase, followed by a slower inactivation phase. A 50-ms prepulse to +80 mV preceding the test pulse (test pulse 2) did not affect the characteristics of this current. In cells co-transfected with $G\beta_1$ and $G\gamma_2$, I_{Ba} inhibition during a single depolarizing test pulse is apparent in the current tracing by the reduced current amplitude and kinetic slowing of activation (Fig. 5, *inset, tracing 1*). The depolarizing prepulse relieves this inhibition by $G\beta_1\gamma_2$, and the resulting facilitation is seen in the increased I_{Ba} during test pulse 2 (Fig. 5, *inset, tracing 2*), compared with test pulse 1. The "facilitation ratio," defined as the ratio of the current amplitude during the peak of test pulse 2 divided by the current during test pulse 1 at the same time point, reflects the magnitude of Gβγ-mediated inhibition of voltage-dependent N-type Ca^{2+} channel currents (26).

Table I and Fig. 5 illustrate the effect of expressing isolated Gβ or Gγ subunits, or combinations of Gβ and Gγ subunits, in C2D7 cells on Ca^{2+} channel facilitation ratios. In cells transfected with GFP and a single Gβ or Gγ subunit, near identical I_{Ba} tracings were obtained during test pulses with and without the depolarizing prepulse, indicating that individual subunits fail to produce voltage-dependent inhibition of N-type Ca^{2+} channels in these cells. In contrast, all tested $G\beta/G\gamma_2$ and $G\beta/G\gamma_{13}$ pairs inhibited these currents, as demonstrated by the significantly enhanced facilitation ratios compared with control (Fig. 5). Notably, however, $G\gamma_{13}$ was less efficacious than $G\gamma_2$ when paired with $G\beta_2$ and $G\beta_5$ in this effector paradigm; in particular, the $G\beta_5/G\gamma_{13}$ pairing yielded a facilitation ratio that was not statistically different from that resulting by $G\gamma_{13}$ transfection alone (Fig. 5).

Activation of PLCβ2 by Gβ/Gγ13 Pairs—Phosphatidylinositol-specific PLCβ isoforms are activated by $G\alpha_{q/11}$ and Gβγ subunits of heterotrimeric G-proteins (31–35); in particular, PLCβ1 is more responsive to $G\alpha_q$ activation than PLCβ2, whereas the opposite is true for Gβγ-mediated activation (36). We therefore examined the ability of $G\gamma_{13}$ to participate in the formation of PLCβ2 activating Gβγ dimers in transfected COS-7 cells. Transfection of $G\beta_1$ with $G\gamma_2$ or $G\gamma_{13}$ promoted ~2-fold increases in [^{3}H]inositol phosphate forma-

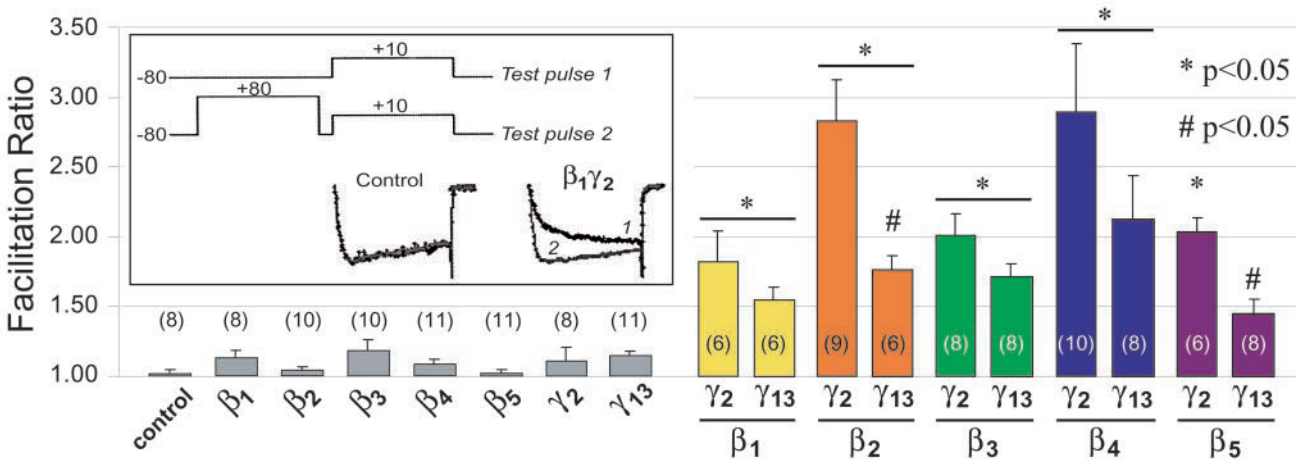

FIG. 5. **Inhibition of N-type Ca^{2+} channels by $G\beta/G\gamma_2$ and $G\beta/G\gamma_{13}$ dimers.** HEK293 cells stably expressing human α_{1B} (N-type) Ca^{2+} channels (α_{1B}, $\alpha_2\delta$, and β_{1-3} subunits; "C2D7" cells) were transiently transfected with $G\beta/G\gamma_2$ or $G\beta/G\gamma_{13}$ expression vector pairs to study their effects on Ca^{2+} channel activity measured by whole cell patch clamp electrophysiological recordings. *Inset*, in untransfected C2D7 cells, a 50-ms depolarizing test pulse to +10 mV ("*test pulse 1*") from a −80 mV holding potential elicited a rapidly activating and slowing inactivating Ba^{2+} current (I_{Ba}) which was not significantly altered by a 50-ms prepulse to +80 mV ("test pulse 2") (26). Expression of functional $G\beta\gamma$ subunits reduced the I_{Ba} amplitude upon test pulse 1 and slows its activation rate; this inhibition was "relieved" by the depolarizing prepulse of test pulse 2. The facilitation ratio, an index of voltage-dependent inhibition of Ca^{2+} channels by $G\beta\gamma$ subunits, is defined as the peak current of test pulse 2 divided by the current of test pulse 1 at the same time point. *Bar graph* depicts facilitation ratios (mean ± S.E.) derived from cells transfected either with single subunit expression vectors (as negative controls) or with indicated $G\beta/G\gamma$ pairs (see Table I). *Numerals* in *parentheses* denote number of cells tested for each transfection paradigm. *Asterisks* (*) denote statistically significant differences from control cells and *number signs* (#) denote statistically significant decreases in facilitation ratio for a particular $G\beta/G\gamma_{13}$ pairing over that observed for matching $G\beta/G\gamma_2$ pairing ($p < 0.05$, one-way ANOVA followed by nonparametric Kolmogorov-Smirnov test ($n = 6–11$)).

TABLE I
Inhibition of N-type Ca^{2+} channels by $G\beta/G\gamma_2$ and $G\beta/G\gamma_{13}$ dimers

Transfection	Number of cells analyzed	Current during test pulse 1	Current during test pulse 2	Facilitation ratio
			pA	
		(mean ± S.E.)	(mean ± S.E.)	(mean ± S.E.)
Control	8	−1983 ± 377	−1951 ± 340	0.99 ± 0.01
β_1	8	−2417 ± 386	−2579 ± 410	1.10 ± 0.06
β_2	10	−2092 ± 401	−2142 ± 403	1.04 ± 0.02
β_3	10	−2540 ± 593	−2768 ± 597	1.17 ± 0.05
β_4	11	−2278 ± 458	−2400 ± 468	1.09 ± 0.04
β_5	11	−1791 ± 748	−1796 ± 771	1.01 ± 0.02
γ_2	8	−1366 ± 309	−1394 ± 306	1.11 ± 0.09
γ_{13}	11	−1331 ± 320	−1470 ± 321	1.15 ± 0.03
$\beta_1\gamma_2$	6	−904 ± 294	−1473 ± 441	1.82 ± 0.22
$\beta_1\gamma_{13}$	6	−638 ± 212	−907 ± 268	1.55 ± 0.09
$\beta_2\gamma_2$	9	−348 ± 67	−1022 ± 243	2.84 ± 0.28
$\beta_2\gamma_{13}$	6	−725 ± 177	−1244 ± 307	1.80 ± 0.10
$\beta_3\gamma_2$	8	−425 ± 106	−791 ± 183	2.01 ± 0.16
$\beta_3\gamma_{13}$	8	−363 ± 119	−646 ± 237	1.70 ± 0.09
$\beta_4\gamma_2$	10	−793 ± 356	−1512 ± 416	2.90 ± 0.48
$\beta_4\gamma_{13}$	8	−1214 ± 389	−2134 ± 594	2.10 ± 0.31
$\beta_5\gamma_2$	6	−785 ± 191	−1606 ± 432	2.04 ± 0.10
$\beta_5\gamma_{13}$	8	−693 ± 140	−926 ± 146	1.45 ± 0.11

tion (Fig. 6), presumably mediated by the endogenous, $G\beta\gamma$-responsive phospholipases constitutively present in COS-7 cells. The additional transfection of PLCβ2 expression vector with either $G\beta^1/G\gamma_2$ or $G\beta_1/G\gamma_{13}$ pairs resulted in similar 6–7-fold enhancements of inositol phosphate formation over that of the $G\beta\gamma$ pairs alone. Likewise, $G\gamma_{13}$ was equally effective as $G\gamma_2$ in activating PLCβ2 when combined with $G\beta_3$ and $G\beta_4$. (It should be noted that expression of $G\beta_3$-containing dimers repeatedly demonstrated only weak activation of PLCβ2; the pcDNA3.1-based human $G\beta_3$ expression vector was sequenced independently in two different laboratories and confirmed to contain the $G\beta_3$ wild-type sequence, discounting the possibility of mutation rendering this $G\beta$ subunit inactive.) In contrast to the similar activation of PLCβ2 observed upon combining either $G\gamma_2$ or $G\gamma_{13}$ with $G\beta_1$, -3, and -4, the $G\beta_2/G\gamma_{13}$ and $G\beta_5/G\gamma_{13}$ pairings did not activate PLCβ_2 to the same degree as the analogous pairings with $G\gamma_2$ (Fig. 6).

Inhibition of $G\alpha_q$-stimulated PLCβ1 Activity by $G\beta/G\gamma_{13}$ Pairs—Since PLCβ1 is relatively insensitive to activation by $G\beta\gamma$, expression of free $G\beta\gamma$ dimers inhibits $G\alpha_q$-mediated PLCβ1 activation, presumably by binding to, and thus sequestering, $G\alpha_q$ in its GDP-bound form (37, 38). Thus, the ability of $G\gamma_{13}$ to bind $G\beta$ subunits and participate in $G\alpha_q$ coupling and sequestration was examined using inhibition of $G\alpha_q$-stimulated PLCβ1 activity as an effector end point. COS-7 cells were transfected with $G\alpha_q$, PLCβ1, and indicated $G\beta$ and/or $G\gamma$ subunit expression vectors and [^{3}H]inositol phosphate accumulation was measured as described above. When paired with $G\beta_{1-4}$, expression of either $G\gamma_2$ or $G\gamma_{13}$ inhibited PLCβ1 activity (Fig. 7), presumably by sequestration of $G\alpha_q$ via heterotrimer formation. In contrast, neither $G\beta_5/G\gamma_2$ nor $G\beta_5/G\gamma_{13}$ in-

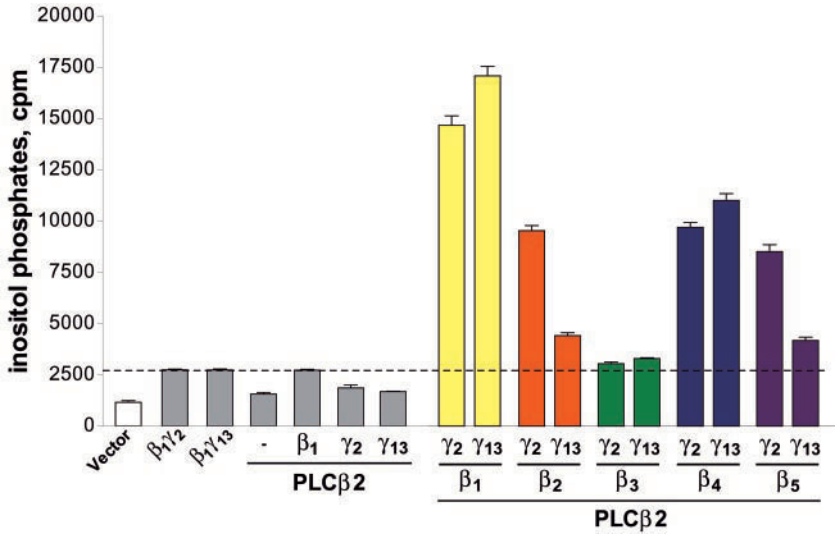

FIG. 6. **Activation of phospholipase PLCβ2 by Gβ/Gγ2 and Gβ/Gγ13 dimers.** COS-7 cells were transiently transfected with PLCβ2 and indicated Gβ and/or Gγ subunit expression vectors, and inositol phosphate accumulation was measured in cells radiolabeled with *myo*-[^{3}H]inositol as described under "Experimental Procedures." Results displayed are representative of three independent experiments; all transfections were performed in triplicate.

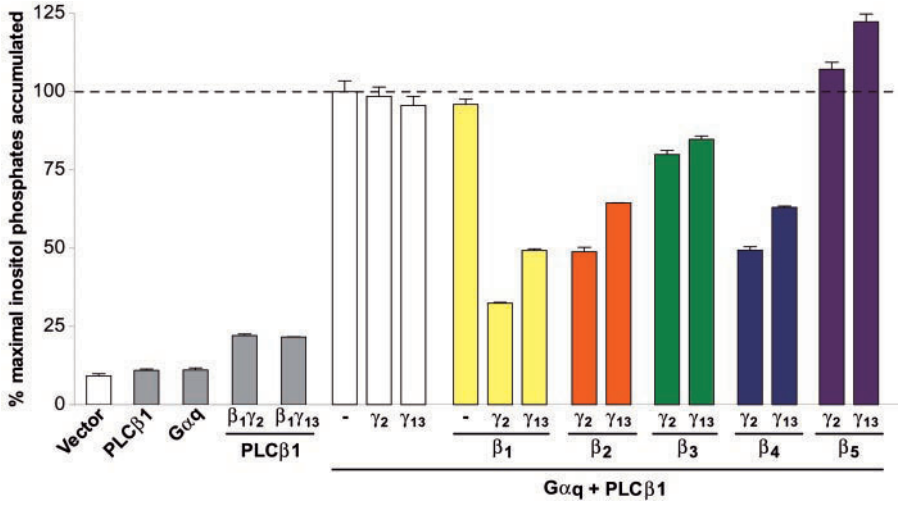

FIG. 7. **Inhibition of $G\alpha_q$-stimulated PLCβ1 activity by Gβ/Gγ2 and Gβ/G_{13} dimers.** COS-7 cells were transiently transfected with $G\alpha_q$, PLCβ1, and indicated Gβ and/or Gγ subunit expression vectors. [^{3}H]Inositol phosphate accumulation was measured as described in the legend to Fig. 6.

hibited $G\alpha_q$-stimulated PLCβ1 activity (Fig. 7). Similarly, $G\beta_{5L}/G\gamma_2$ and $G\beta_{5L}/G\gamma_{13}$ pairings also failed to inhibit $G\alpha_q$-stimulated PLCβ1 activity (data not shown).

DISCUSSION

All of the functional assays of $G\beta/G\gamma_{13}$ dimer activity presented here indicate that the divergent, NPW motif-containing $G\gamma_{13}$ polypeptide is capable of interacting with all five Gβ subunits to varying degrees (summarized in Table II). Moreover, all five $G\beta/G\gamma_{13}$ combinations are capable of forming dimers upon coincident translation *in vitro*. Thus, our initial speculation that $G\gamma_{13}$ might selectively associate with $G\beta_5$, the outlier Gβ isotype that also exhibits a largely neural expression pattern (7, 8), is not supported by our results.

In contrast to our results on *in vitro* dimer assembly and cellular dimer activity, we were unable to detect stable $G\beta_2/G\gamma_{13}$ or $G\beta_5/G\gamma_{13}$ dimers in the lysates of cells co-transfected with expression vectors for these Gβ and Gγ subunits. We believe the inability to detect $G\beta_2/G\gamma_{13}$ or $G\beta_5/G\gamma_{13}$ dimers by cellular co-immunoprecipitation results from enhanced detergent sensitivity that leads to dimer disruption under high-detergent cell lysis and immunoprecipitation conditions. This hypothesis stems from our previous work (21, 23), and that of Garrison and co-workers (39, 40), detailing the uniquely sensitive nature of the $G\beta_5/G\gamma_2$ dimer to low levels of detergent that do not disrupt other conventional $G\beta\gamma$ dimers or $G\beta_5$-GGL complexes (*e.g.* $G\beta_5/G\gamma_2$ dimer disruption by sodium cholate in excess of ~0.25%; Ref. 40). Such a qualitative difference in dimer stability is not only manifest in the apparent detergent sensitivity of $G\beta_2/G\gamma_{13}$ and $G\beta_5/G\gamma_{13}$ dimers, but also in the reduced efficacy of Ca^{2+} channel inhibition and PLCβ_2 activation seen upon $G\beta_2/G\gamma_{13}$ or $G\beta_5/G\gamma_{13}$ co-expression *versus* cognate $G\beta/G\gamma_2$ pairings. The structural basis for this qualitative difference remains undefined.

The selective modulation of effector functions exhibited by $G\beta_5/G\gamma_{13}$ is, with a single exception, consistent with previous studies employing $G\beta_5/G\gamma_2$ dimers (reviewed in Ref. 19). The $G\beta_5/G\gamma_2$ dimer has been shown to activate PLCβ2 (7, 8) and inhibit both Kir3 channels (24) and N-type Ca^{2+} channels (26,

TABLE II
Summary of Gβ association and effector interaction selectivities of $G\gamma_{13}$

$G\beta/G\gamma_{13}$ Functional Assay:	Gβ subunit partner				
	$G\beta_1$	$G\beta_2$	$G\beta_3$	$G\beta_4$	$G\beta_5$
In vitro co-immunoprecipitation	+	+	+	+	+
Cellular co-immunoprecipitation	+	−	+	+	−
Inhibition of N-type Ca^{2+} channels	+	+[a]	+	+	+/−[a,b]
Activation of PLCβ2	+	+[a]	+/−	+	+[a]
Modulation of Kir3.1/3.4 channels[c]	↑	↑	↑	↑	↓
Inhibition of $G\alpha_q$-stimulated PLCβ1	+	+	+	+	−

[a] $G\beta/G\gamma_{13}$ dimer is significantly less active than cognate $G\beta/G\gamma_2$ dimer.

[b] $G\beta_5/G\gamma_{13}$ dimer activity is not significantly different than $G\gamma_{13}$ alone.

[c] Up arrow (↑) denotes increased K_+ conductance; down arrow (↓) denotes decreased conductance.

41), consistent with our findings here using $G\beta_5/G\gamma_{13}$. The observed lack of statistically significant inhibition of N-type Ca^{2+} channels by $G\beta_5/G\gamma_{13}$ over $G\gamma_{13}$ transfection alone may reflect a need for higher amounts of $G\beta_5$ and $G\gamma_{13}$ expression to attain robust channel inhibition *versus* other Gβ/Gγ pairs, a phenomenon first shown by Ruiz-Velasco and Ikeda (41) for the $G\beta_5/G\gamma_2$ dimer.

The single exception is our finding that $G\beta_5/G\gamma_2$ and $G\beta_5/G\gamma_{13}$ dimers are unable to inhibit $G\alpha_q$-mediated activation of PLCβ1 in transfected cells. This is in contrast to the findings of Garrison and colleagues (39) that $G\beta_5/G\gamma_2$ interacts with $G\alpha_q$ in measurements of *in vitro* heterotrimer formation and *in vitro* coupling to M_1 muscarinic and ET_B endothelin receptors (42). While recombinant $G\beta_5/G\gamma_2$ dimers may interact with $G\alpha_q$ *in vitro*, this interaction may be too weak in affinity within a cellular context to affect PLCβ1 activation. Moreover, as we have previously postulated (19), the existence of GGL domains as avid, native binding partners for $G\beta_5$ implies that heterodimers between $G\beta_5$ and conventional Gγ subunits could merely represent unnatural and weakly associated dimers that only inadvertently affect some conventional Gβγ effector systems.

Clearly, our results demonstrate that the functional range of $G\gamma_{13}$ assembly with Gβ subunits is wider than our original conjecture of strict $G\beta_5$ specificity. Thus, the presence of an NPW motif is *not* predictive of exclusive association solely with $G\beta_5$ isoforms, a selectivity previously seen with the NPW motif-containing GGL domains of RGS proteins (19). We are pursuing experimentally derived atomic resolution structural data on the $G\beta_5$/GGL interface with the goal of identifying the residue(s) within the Gγ-like polypeptide responsible for exclusive $G\beta_5$ association and thus refining our Trp-274 hypothesis (21).

Our formal demonstrations of stable $G\beta_3/G\gamma_{13}$ dimer formation using both *in vitro* and cellular co-immunoprecipitations confirm one of the speculations of Huang and colleagues (17) who, in their original report on the cloning of $G\gamma_{13}$, demonstrated fully coincident expression of $G\beta_3$ and $G\gamma_{13}$ mRNAs in murine taste receptor cells but were unable to demonstrate $G\beta_3/G\gamma_{13}$ dimer assembly for technical reasons. However, our results indicate that $G\beta_3/G\gamma_{13}$ activates PLCβ2 weakly if at all, which is consistent with a previous report (43) using other $G\beta_3$/Gγ combinations but runs counter to the speculation by Huang and colleagues (17) that $G\beta_3/G\gamma_{13}$ is responsible for PLCβ2 activation in bitter taste signal transduction. As one explanation for this discrepancy, the bitter taste response has been suggested to rely on a "unique" PLCβ2 isoform which is specifically expressed in taste receptor cells (44) yet remains functionally uncharacterized.

$G\gamma_{13}$ was originally cloned from taste receptor cells and co-localized with *Gα-gustducin*, $G\beta_1$, and $G\beta_3$ transcripts within mouse circumvallate papillae (17); these results led Huang and colleagues (17) to suggest that $G\gamma_{13}$, as part of a gustducin heterotrimer, participates in bitter and sweet taste signal transduction via $G\beta_1/G\gamma_{13}$- or $G\beta_3/G\gamma_{13}$-mediated PLCβ activation. Our results demonstrating $G\gamma_{13}$ expression in the central nervous system, as well as association of $G\gamma_{13}$ with all five Gβ subunits, imply that the functional roles for $G\gamma_{13}$ extend beyond taste reception. The next challenge will be to define precisely these other locales and other roles for $G\gamma_{13}$ and determine whether the divergent nature of its polypeptide sequence affects its function in receptor coupling and downstream signaling compared with more conventional Gγ subunits.

Acknowledgments—Special thanks to Dr. John Sondek, Jason Snyder, and Randall Kimple for technical support and Dr. Miller B. Jones for comments on this manuscript. One of us (B. L. B.) thanks Dr. Richard Mailman, under whose mentorship this project was initiated.

REFERENCES

1. Gilman, A. G. (1987) *Annu. Rev. Biochem.* **56,** 615–649
2. Hamm, H. E. (1998) *J. Biol. Chem.* **273,** 669–672
3. Clapham, D. E., and Neer, E. J. (1997) *Annu. Rev. Pharmacol. Toxicol.* **37,** 167–203
4. Schwindinger, W. F., and Robishaw, J. D. (2001) *Oncogene* **20,** 1653–1660
5. Hildebrandt, J. D. (1997) *Biochem. Pharmacol.* **54,** 325–339
6. Gautam, N., Downes, G. B., Yan, K., and Kisselev, O. (1998) *Cell. Signal.* **10,** 447–455
7. Watson, A. J., Katz, A., and Simon, M. I. (1994) *J. Biol. Chem.* **269,** 22150–22156
8. Watson, A. J., Aragay, A. M., Slepak, V. Z., and Simon, M. I. (1996) *J. Biol. Chem.* **271,** 28154–28160
9. Fawzi, A. B., Fay, D. S., Murphy, E. A., Tamir, H., Erdos, J. J., and Northup, J. K. (1991) *J. Biol. Chem.* **266,** 12194–12200
10. Kisselev, O. G., Ermolaeva, M. V., and Gautam, N. (1994) *J. Biol. Chem.* **269,** 21399–21402
11. Matsuda, T., Hashimoto, Y., Ueda, H., Asano, T., Matsuura, Y., Doi, T., Takao, T., Shimonishi, Y., and Fukada, Y. (1998) *Biochemistry* **37,** 9843–9850
12. Myung, C. S., Yasuda, H., Liu, W. W., Harden, T. K., and Garrison, J. C. (1999) *J. Biol. Chem.* **274,** 16595–16603
13. Wall, M. A., Coleman, D. E., Lee, E., Iniguez-Lluhi, J. A., Posner, B. A., Gilman, A. G., and Sprang, S. R. (1995) *Cell* **83,** 1047–1058
14. Sondek, J., Bohm, A., Lambright, D. G., Hamm, H. E., and Sigler, P. B. (1996) *Nature* **379,** 369–374
15. Lambright, D. G., Sondek, J., Bohm, A., Skiba, N. P., Hamm, H. E., and Sigler, P. B. (1996) *Nature* **379,** 311–319
16. Wall, M. A., Posner, B. A., and Sprang, S. R. (1998) *Structure* **6,** 1169–1183
17. Huang, L., Shanker, Y. G., Dubauskaite, J., Zheng, J. Z., Yan, W., Rosenzweig, S., Spielman, A. I., Max, M., and Margolskee, R. F. (1999) *Nat. Neurosci.* **2,** 1055–1062
18. Inoue, S., Sano, H., and Ohta, M. (2000) *Biochem. Biophys. Res. Commun.* **268,** 553–561
19. Sondek, J., and Siderovski, D. P. (2001) *Biochem. Pharmacol.* **61,** 1329–1337
20. Snow, B. E., Krumins, A. M., Brothers, G. M., Lee, S. F., Wall, M. A., Chung, S., Mangion, J., Arya, S., Gilman, A. G., and Siderovski, D. P. (1998) *Proc. Natl. Acad. Sci. U. S. A.* **95,** 13307–13312
21. Snow, B. E., Betts, L., Mangion, J., Sondek, J., and Siderovski, D. P. (1999) *Proc. Natl. Acad. Sci. U. S. A.* **96,** 6489–6494
22. Evanko, D. S., Thiyagarajan, M. M., Siderovski, D. P., and Wedegaertner, P. B. (2001) *J. Biol. Chem.* **276,** 23945–23953
23. Siderovski, D. P., Snow, B. E., Chung, S., Brothers, G. M., Sondek, J., and Betts, L. (2001) *Methods Enzymol.* **344,** 702–723
24. Lei, Q., Jones, M. B., Talley, E. M., Schrier, A. D., McIntire, W. E., Garrison, J. C., and Bayliss, D. A. (2000) *Proc. Natl. Acad. Sci. U. S. A.* **97,** 9771–9776
25. Simen, A. A., and Miller, R. J. (1998) *J. Neurosci.* **18,** 3689–3698
26. Zhou, J. Y., Siderovski, D. P., and Miller, R. J. (2000) *J. Neurosci.* **20,** 7143–7148
27. Schultz, J., Copley, R. R., Doerks, T., Ponting, C. P., and Bork, P. (2000) *Nucleic Acids Res.* **28,** 231–234
28. Adams, M. D., et al. (2000) *Science* **287,** 2185–2195
29. Schulz, S., Huber, A., Schwab, K., and Paulsen, R. (1999) *J. Biol. Chem.* **274,** 37605–37610
30. Schuler, G. D. (1997) *J. Mol. Med.* **75,** 694–698
31. Taylor, S. J., Chae, H. Z., Rhee, S. G., and Exton, J. H. (1991) *Nature* **350,** 516–518
32. Boyer, J. L., Waldo, G. L., and Harden, T. K. (1992) *J. Biol. Chem.* **267,** 25451–25456
33. Wu, D., Katz, A., Lee, C. H., and Simon, M. I. (1992) *J. Biol. Chem.* **267,** 25798–25802
34. Katz, A., Wu, D., and Simon, M. I. (1992) *Nature* **360,** 686–689
35. Camps, M., Carozzi, A., Schnabel, P., Scheer, A., Parker, P. J., and Gierschik, P. (1992) *Nature* **360,** 684–686
36. Paterson, A., Boyer, J. L., Watts, V. J., Morris, A. J., Price, E. M., and Harden, T. K. (1995) *Cell. Signal.* **7,** 709–720
37. Smrcka, A. V., and Sternweis, P. C. (1993) *J. Biol. Chem.* **268,** 9667–9674
38. Boyer, J. L., Graber, S. G., Waldo, G. L., Harden, T. K., and Garrison, J. C. (1994) *J. Biol. Chem.* **269,** 2814–2819
39. Fletcher, J. E., Lindorfer, M. A., DeFilippo, J. M., Yasuda, H., Guilmard, M., and Garrison, J. C. (1998) *J. Biol. Chem.* **273,** 636–644
40. Jones, M. B., and Garrison, J. C. (1999) *Anal. Biochem.* **268,** 126–133
41. Ruiz-Velasco, V., and Ikeda, S. R. (2000) *J. Neurosci.* **20,** 2183–2191
42. Lindorfer, M. A., Myung, C. S., Savino, Y., Yasuda, H., Khazan, R., and Garrison, J. C. (1998) *J. Biol. Chem.* **273,** 34429–34436
43. Hawes, B. E., van Biesen, T., Koch, W. J., Luttrell, L. M., and Lefkowitz, R. J. (1995) *J. Biol. Chem.* **270,** 17148–17153
44. Rossler, P., Kroner, C., Freitag, J., Noe, J., and Breer, H. (1998) *Eur. J. Cell. Biol.* **77,** 253–261
45. Moores, S. L., Schaber, M. D., Mosser, S. D., Rands, E., O'Hara, M. B., Garsky, V. M., Marshall, M. S., Pompliano, D. L., and Gibbs, J. B. (1991) *J. Biol. Chem.* **266,** 14603–14610
46. Ray, K., Kunsch, C., Bonner, L. M., and Robishaw, J. D. (1995) *J. Biol. Chem.* **270,** 21765–21771